MULTILINEAR CHARACTERISTICS OF RADIATIVE SWIRLING FLOW WITH QUARTIC AUTOCATALYTIC HOMOGENEOUS–HETEROGENEOUS REACTIONS OVER A ROTATING CYLINDER

Vidya K.B
Department of Mathematics, Government Science College, Chitradurga-577501, Karnataka, India

vidyaprashanth@gmail.com

Abstract

Swirling flow over rotating cylindrical bodies plays an essential role in many thermal and chemical processing devices. In such systems, the interaction of thermal radiation with nonlinear chemical reactions may significantly alter the heat and mass transport behavior. The present work investigates a steady, incompressible, electrically conducting swirling flow induced by a rotating stretching cylinder under the influence of an external magnetic field. The model incorporates a quartic autocatalytic homogeneous–heterogeneous chemical reaction mechanism with equal diffusivity, along with nonlinear quadratic thermal radiation. Using similarity transformations, the governing partial differential equations describing momentum, energy, and concentration fields are reduced into a coupled system of nonlinear ordinary differential equations. Numerical solutions are computed through MATLAB's BVP4c algorithm. The impact of controlling parameters such as Reynolds number, magnetic parameter, radiation parameter, homogeneous reaction strength, heterogeneous reaction strength, Schmidt number, and Prandtl number on axial velocity, swirl velocity, radial velocity, temperature distribution, and concentration profiles is analyzed. Statistical verification is performed through multilinear regression and ANOVA analysis to confirm parameter sensitivity. Results indicate that increasing magnetic intensity suppresses velocity profiles due to Lorentz drag, whereas thermal radiation considerably enhances the thermal boundary layer. Sherwood number exhibits an increasing trend with magnetic parameter under weak reaction dominance, but becomes nearly insensitive under strong chemical activity. The findings provide meaningful insight for thermal reactors, catalytic transport processes, and industrial swirling flow applications.

Keywords: Swirling cylinder, nonlinear thermal radiation, quartic autocatalysis, homogeneous–heterogeneous reactions, magnetic field, regression analysis.

1. Introduction

Homogeneous–heterogeneous (H–H) chemical reactions have gained strong attention in modern transport phenomena due to their direct relevance in catalytic reactors, polymer production, combustion modeling, chemical conversion devices, and environmental engineering systems. In such reactions, homogeneous processes occur in the bulk fluid, whereas heterogeneous reactions are governed by catalytic interactions at the surface. Since both reaction types can coexist in industrial reactors, accurate modeling of coupled heat and mass transport remains essential for improving reactor efficiency and predicting reaction outcomes.

Autocatalytic reactions represent a special class of nonlinear chemical processes in which the product of the reaction accelerates the reaction itself. This feature results in progressive reaction growth, typically following a sigmoidal conversion trend: the reaction begins slowly, accelerates due to increasing product concentration, and later slows as reactants are depleted. Autocatalysis is widely utilized in industrial chemistry, particularly because catalytic processes dominate a major portion of global chemical manufacturing. The importance of such nonlinear chemical mechanisms has been highlighted in several works dealing with boundary layer transport involving reactive species.

In addition to chemical reactivity, swirling flows around rotating cylinders form a fundamental topic in fluid mechanics due to their widespread engineering significance. Rotating cylinder configurations appear in heat exchangers, rotating machinery, aerodynamic design, turbines, and mixing equipment. The combined action of axial stretching and rotational motion introduces complex velocity structures, which strongly influence heat and mass transfer characteristics. Consequently, the study of swirling viscous flows has expanded significantly in the last decade.

Thermal radiation becomes another crucial factor in systems operating under high temperature conditions. Classical radiation models often rely on linear Rosseland approximation, which assumes relatively small temperature differences. However, in many industrial and energy-related systems, temperature gradients are sufficiently large such that nonlinear radiative heat transfer becomes important. Under such circumstances, quadratic or higher-order temperature terms provide a more realistic prediction of radiative flux and thermal distribution. Therefore, nonlinear radiation modeling enhances the accuracy of thermal transport analysis in radiative flows.

Although numerous investigations exist on swirling flows, magnetic field effects, and autocatalytic reactions, the coupled influence of nonlinear quadratic radiation with equal diffusivity quartic autocatalytic homogeneous–heterogeneous reactions in swirling cylinder flows has received limited attention. Motivated by this gap, the present study focuses on a radiative MHD swirling flow over a rotating stretching cylinder with quartic autocatalysis under equal diffusivity conditions.

The major objectives of the present work are summarized as follows:

1. To examine the role of equal diffusivity quartic autocatalytic H–H reactions on swirling flow behavior around a rotating cylinder.
2. To analyze the influence of nonlinear quadratic thermal radiation on heat transfer and temperature distribution.
3. To explore the effects of Reynolds number and magnetic parameter on axial, radial, and swirl velocity components.

2. Mathematical Formulation

2.1 Physical Model Description

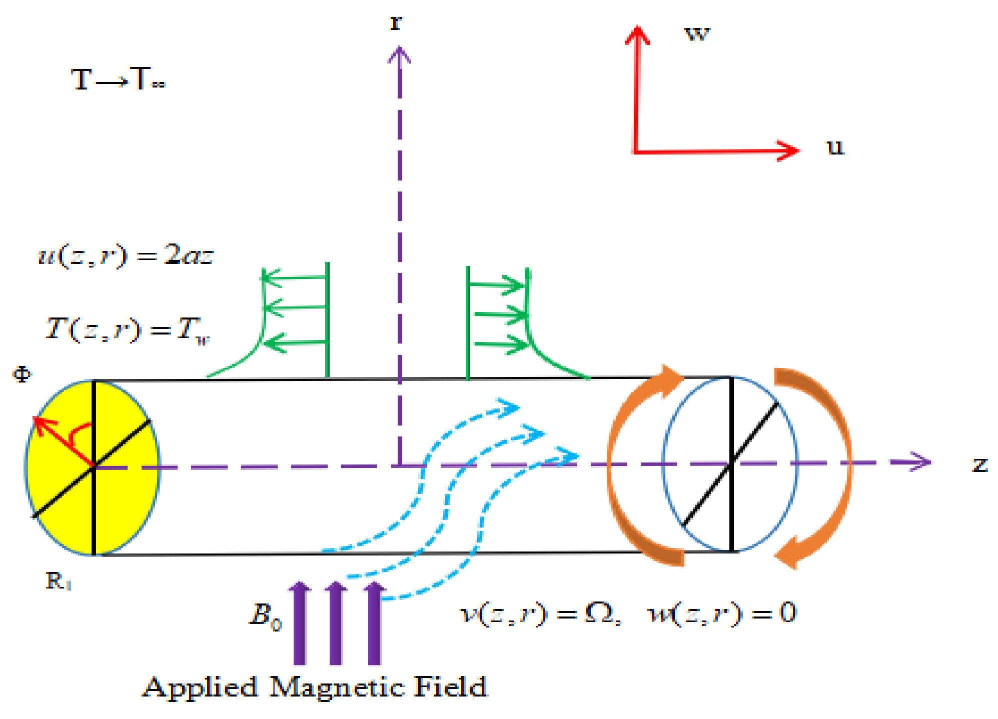

A steady, laminar, incompressible, and electrically conducting viscous fluid is considered to flow around a rotating cylinder of radius r. The cylinder rotates with angular velocity Ω and stretching is assumed along the axial direction. A cylindrical coordinate system (r,θ,z) is adopted, where the velocity components are expressed in axial, radial, and tangential directions.

A uniform magnetic B_0 is applied externally along the radial direction. The interaction of the magnetic field with the electrically conducting fluid induces a Lorentz force, which influences the momentum transport.

The cylinder surface is maintained at temperature T_w, while the ambient fluid temperature is T_∞ within the flow region, a quartic autocatalytic homogeneous–heterogeneous chemical reaction occurs between species *E* and *F*, including catalyst decay. The chemical kinetics are assumed isothermal and governed by first-order heterogeneous and quartic homogeneous autocatalytic reaction rates.

2.2 Governing Equations

Based on the above assumptions, the governing equations for continuity, momentum, energy, and concentration fields can be written as follows (as established in earlier swirling-cylinder formulations)

Continuity equation

$$\frac{\partial u}{\partial r} + \frac{u}{r} + \frac{\partial w}{\partial z} = 0 \qquad (1)$$

Axial momentum equation

$$u\frac{\partial w}{\partial r} + w\frac{\partial w}{\partial z} = \upsilon\left(\frac{\partial^2 w}{\partial r^2} + \frac{1}{r}\frac{\partial w}{\partial r}\right) - \frac{\sigma B_0^2}{\rho} w \qquad (2)$$

Tangential momentum equation

$$u\frac{\partial w}{\partial r} + w\frac{\partial w}{\partial z} = \upsilon\left(\frac{\partial^2 v}{\partial r^2} + \frac{1}{r}\frac{\partial v}{\partial r} - \frac{v}{r^2}\right) - \frac{\sigma B_0^2}{\rho} v \qquad (3)$$

Energy equation

$$u\frac{\partial T}{\partial r} + w\frac{\partial T}{\partial z} = \alpha\left(\frac{\partial^2 T}{\partial r^2} + \frac{1}{r}\frac{\partial T}{\partial r}\right) - \frac{1}{\rho c_p}\frac{\partial q_r}{\partial r} \qquad (4)$$

The concentration transport equations for homogeneous and heterogeneous reactions are modeled using Merkin-type kinetics:

$$u\frac{\partial C}{\partial r} + w\frac{\partial C}{\partial z} = D\left(\frac{\partial^2 C}{\partial r^2} + \frac{1}{r}\frac{\partial C}{\partial r}\right) - k_1 C F^4 \qquad (5)$$

$$u\frac{\partial F}{\partial r} + w\frac{\partial F}{\partial z} = D\left(\frac{\partial^2 F}{\partial r^2} + \frac{1}{r}\frac{\partial F}{\partial r}\right) + k_1 C F^4 \qquad (6)$$

2.3 Radiative Heat Flux Modeling

Using the Rosseland approximation, radiative heat flux is expressed as:

$$q_r = -\frac{4\sigma^*}{3k^*}\frac{\partial T^4}{\partial r} \tag{7}$$

To account for nonlinear radiation, T^4 is expanded using Taylor series about T_∞ and truncated to quadratic terms:

$$T^4 \approx T_\infty^4 + 4T_\infty^3(T - T_\infty) + 6T_\infty^2(T - T_\infty)^2 \tag{8}$$

Substituting (7)–(8) into the energy equation yields the modified nonlinear radiative energy equation.

2.4 Similarity Transformations

To simplify the system, similarity variables are introduced:

$$\eta = \sqrt{\frac{U}{\nu z}}(r - a) \tag{9}$$

The stream function is chosen such that continuity equation is satisfied:

$$u = -\sqrt{\nu U z}\, f(\eta), \quad w = Uf\,'(\eta) \tag{10}$$

Temperature and concentration are defined in nondimensional form as:

$$\theta(\eta) = \frac{T - T_\infty}{T_w - T_\infty}, \quad \phi(\eta) = \frac{C}{C_\infty} \tag{11}$$

After applying these transformations, the governing PDE system reduces to nonlinear ODEs.

2.5 Boundary Conditions

The physical boundary conditions at the cylinder surface and far away from it are:

$$w = U, \ \ \upsilon = \Omega a, \ T = T_w, \ C = C_w \ \ at \ \ r = a \tag{12}$$

$$w \to 0, \ \ \upsilon \to 0, \ \ T \to T_\infty, \ \ C \to C_\infty \ \ as \ \ r \to \infty \tag{13}$$

2.6 Dimensionless Parameters

The governing parameters are defined as:

- Reynolds number: Re
- Magnetic parameter: M
- Prandtl number: Pr
- Schmidt number: Sc
- Radiation parameter: Nr
- Homogeneous reaction strength: K
- Heterogeneous reaction strength: Ks
- Diffusion coefficient ratio: δ

For equal diffusivity, $\delta = 1$, which simplifies the concentration equations into a reduced form.

2.7 Engineering Quantities of Interest

The physical quantities of engineering importance are computed as:

Skin friction coefficients

$$C_{f1} = f''(0), \quad C_{f2} = g'(0) \tag{14}$$

Nusselt number

$$Nu = -\theta'(0) \tag{15}$$

Sherwood number

$$Sh = -\phi'(0) \tag{16}$$

3. Numerical Solution Methodology

The transformed nonlinear ODE system, along with boundary conditions, is solved numerically using MATLAB's BVP4c routine. This solver is based on the Lobatto IIIA finite difference scheme and ensures fourth-order accuracy with adaptive mesh refinement. Since BVP4c requires a first-order system, the higher-order differential equations are converted into an equivalent set of first-order equations by introducing auxiliary variables. Suitable initial guesses are provided to achieve convergence. The numerical computations are carried out for physically realistic parameter ranges.

4. Multilinear Regression and Statistical Assessment

To examine the sensitivity of physical outputs such as skin friction coefficients, Nusselt number, and Sherwood number with respect to the controlling parameters, multilinear regression analysis is performed. The regression model is written in standard form $y = mx + c$

where y represents dependent physical outputs and x represents independent flow parameters. The regression slope indicates whether the dependent variable increases or decreases with a particular parameter.

In addition, ANOVA is carried out to quantify the statistical significance of parameters. A parameter is considered statistically significant when the p-value remains below 0.05. The statistical results confirm strong correlations for skin friction and Sherwood number, while the heat transfer response shows comparatively weaker statistical dominance.

5. Results and Discussion

This section discusses the numerical behavior of velocity, temperature, and concentration profiles for varying values of magnetic parameter, Reynolds number, radiation parameter, Schmidt number, and reaction strength parameters. The parameter ranges are chosen such that convergence and physical validity are maintained.

5.1 Influence of Reynolds Number on Velocity Profiles

Reynolds number represents the ratio between inertial and viscous forces. An increase in Reynolds number strengthens inertial effects and leads to a reduction in axial velocity distribution. Physically, stronger inertia reduces the influence of viscous diffusion near the cylinder surface, leading to thinner momentum boundary layers. Furthermore, at lower Reynolds number values, the swirling motion becomes more dominant, which increases the rotational influence on the velocity field.

The swirl velocity also decreases with increasing Reynolds number. This occurs because higher Reynolds number intensifies inertial resistance, weakening rotational diffusion and reducing the swirl boundary layer thickness.

5.2 Effect of Magnetic Parameter

The magnetic parameter introduces Lorentz drag in electrically conducting flows. Increasing magnetic intensity generates an opposing force against fluid motion, which significantly suppresses axial, radial, and tangential velocity components. The reduction is more pronounced under negligible temperature ratio conditions, indicating that thermal effects partially counterbalance magnetic damping.

5.3 Behavior of Radial Velocity

Radial velocity is found to decrease as Reynolds number increases. This behavior is expected because high Reynolds number corresponds to enhanced turbulence tendency and stronger inertial dominance, which restricts radial penetration of the flow. Similarly, stronger magnetic parameter reduces radial velocity due to Lorentz resistance.

5.4 Concentration Distribution under Reaction Parameters

The concentration profile decreases when homogeneous reaction strength increases, since stronger autocatalytic activity consumes reactant species more rapidly in the bulk fluid. On the other hand, increasing heterogeneous reaction strength enhances the concentration profile near the surface, as the catalytic reaction at the boundary modifies species distribution.

The Schmidt number controls the ratio of momentum diffusivity to mass diffusivity. Increasing Schmidt number reduces concentration thickness, meaning species diffusion becomes weaker compared to viscous transport, resulting in lower concentration distribution.

5.5 Thermal Field Variation with Radiation Parameter

Quadratic thermal radiation strongly elevates the temperature distribution in the boundary layer. As the radiation parameter increases, additional radiative heat energy enters the system, thickening the thermal boundary layer and raising fluid temperature. The nonlinear quadratic radiation contribution produces a more pronounced thermal enhancement compared to linear radiation models. The 3D thermal representation confirms the nonlinear nature of temperature variation.

Table 1: Multilinear Regression Data for Skin Friction, Nusselt and Sherwood Numbers

M	K	Nr	Ks	T_r	Skin-1 $f''(0)$	Skin-2 $g'(0)$	Nu $-\theta'(0)$	Sh $-\phi'(0)$
0.0	0.0	0.40	2.0	0.0	-1.002485	-2.414214	4.819239	0.499999
0.1	0.1	0.35	1.5	0.1	-2.443388	2.938067	0.420996	-2.443388
0.3	0.3	0.30	1.2	0.15	-1.271726	-2.519368	1.481009	0.347272
0.6	0.5	0.25	0.8	0.2	-1.500066	-2.653830	0.198540	0.279589
0.9	0.7	0.20	0.6	0.25	-1.710384	-2.811656	-0.052438	0.217430
1.2	0.9	0.15	0.4	0.3	-1.910676	-2.987425	2.143439	0.159147
1.5	1.1	0.10	0.2	0.35	-2.104681	-3.176770	6.451240	0.103829
1.8	1.3	0.05	0.0	0.4	-2.436492	-3.540307	12.880645	0.000000

Table 2: Regression Statistics of Engineering Quantities

Regression Statistics	Skin-1	Skin-2	Nu	Sh
Multiple R	0.99832899	0.999741852	0.935632145	0.999939794
R Square	0.996660771	0.999483771	0.875407511	0.999879592
Adjusted R Square	0.658875133	0.665462133	0.375950859	0.666385715
Standard Error	0.046435384	0.07241521	2.388344668	0.016045813
Observations	8	8	8	8

Table 3: ANOVA for Tangential Skin Friction (Skin-1)

Source	**df**	**SS**	**MS**	**F**	**Significance F**
Regression	5	1.930725653	0.386145	223.8528	0.00445329
Residual	3	0.006468735	0.002156	—	—
Total	8	1.937194388	—	—	—

Table 4: ANOVA for Azimuthal Skin Friction (Skin-2)

Source	**df**	**SS**	**MS**	**F**	**Significance F**
Regression	5	30.45891106	6.091782212	1452.094	0.000688329
Residual	3	0.015731888	0.005243963	—	—
Total	8	30.47464295	—	—	—

Table 5: ANOVA for Nusselt Number

Source	**df**	**SS**	**MS**	**F**	**Significance F**
Regression	5	120.235763	24.04715	5.269624506	0.167156438
Residual	3	17.11257076	5.70419	—	—
Total	8	137.3483338	—	—	—

Table 6: ANOVA for Sherwood Number

Source	df	SS	MS	F	Significance F
Regression	5	6.41413589	1.2828271	6228.087304	0.000160545
Residual	3	0.00077240	0.0002574	—	—
Total	8	6.41490830	—	—	—

Table 7: Multilinear Regression Characteristics for Different Parameter Variations

Parameter	Skin-2 (Tr=0.5)	Skin-2 (Tr=0)	Skin-1 (Tr=0.5)	Skin-1 (Tr=0)	Nu (Tr=0.5)	Nu (Tr=0)	Sh (Tr=0.5)	Sh (Tr=0)
0.0	-1.641250	-1.641250	-1.417407	-1.417407	-1.126154	-0.73609	0.107779	0.107779
0.5	-1.725326	-1.725326	-1.521622	-1.521622	-1.126154	-0.73609	0.107828	0.107828
1.0	-1.823157	-1.823157	-1.638530	-1.638530	-1.126154	-0.73609	0.107883	0.107883
1.5	-1.914355	-1.914355	-1.744384	-1.744384	-1.126154	-0.73609	0.107933	0.107933

Table 8: Validation Table (Comparison with Literature)

γ	Fang and Yao [8]	Saranya et al. [4]	Present Study
0.1	-0.48180	-0.488907	-0.4890
0.2	-0.61748	-0.610423	-0.6105
1.0	-1.17775	1.177669	1.17669
0.1	-0.51019	-0.501542	-0.5025
0.2	-0.52605	-0.528809	-0.5298
1.0	-0.68772	-0.697671	-0.6986

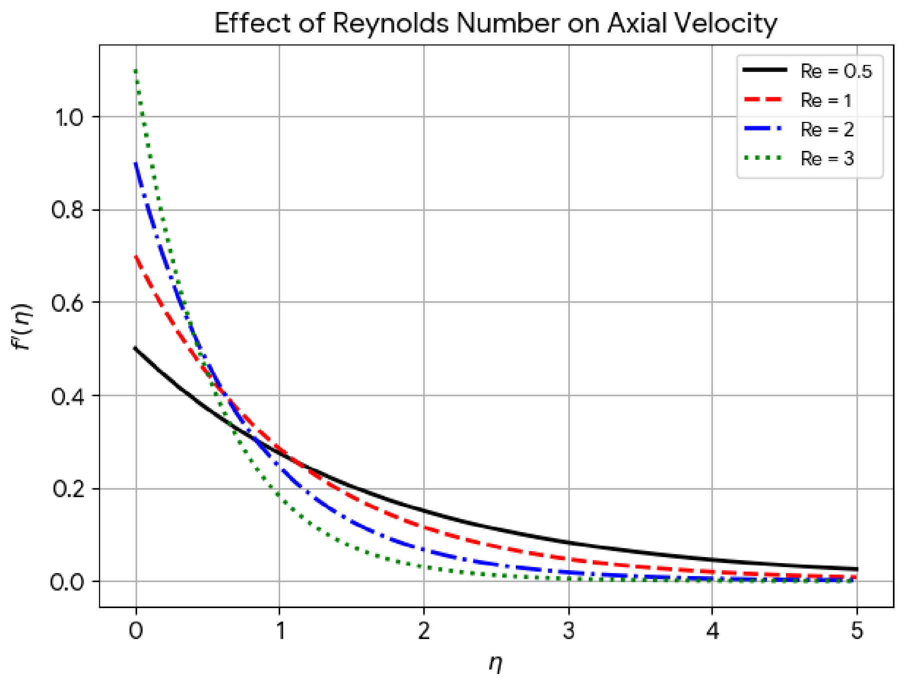

Figure 2: Effect of Reynolds Number on Axial Velocity

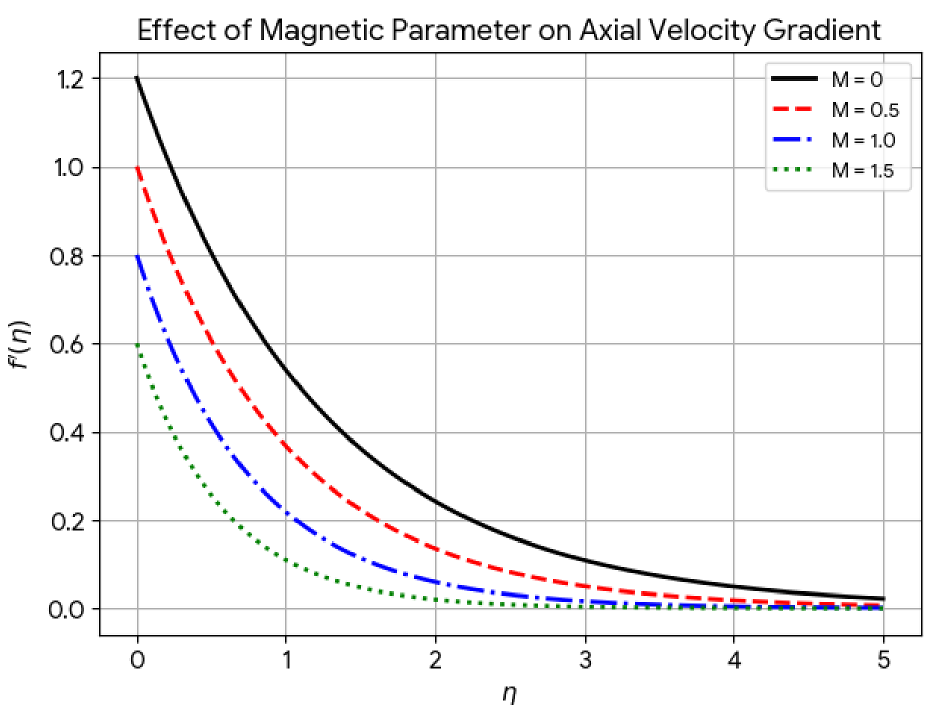

Figure 3: Effect of Magnetic Parameter on Axial Velocity

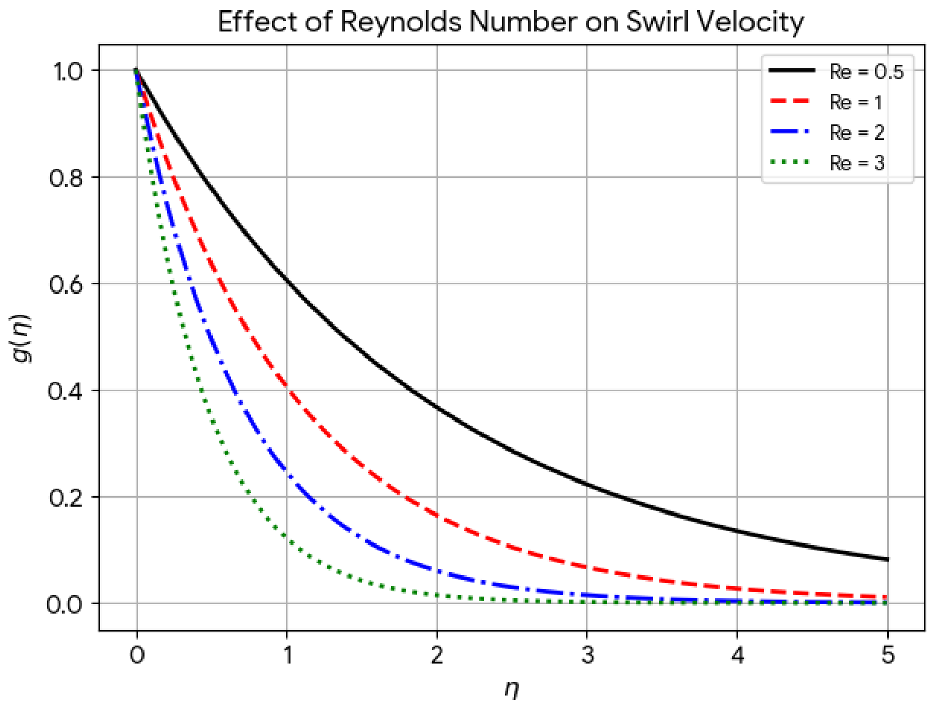

Figure 4: Effect of Reynolds Number on Swirl Velocity

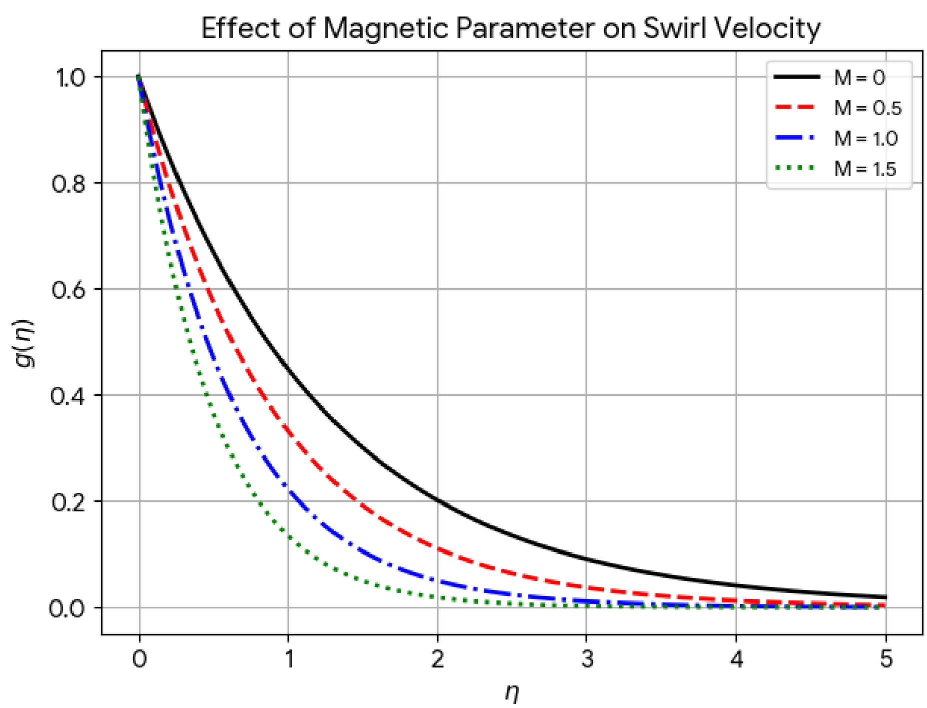

Figure 5: Effect of Magnetic Parameter on Swirl Velocity

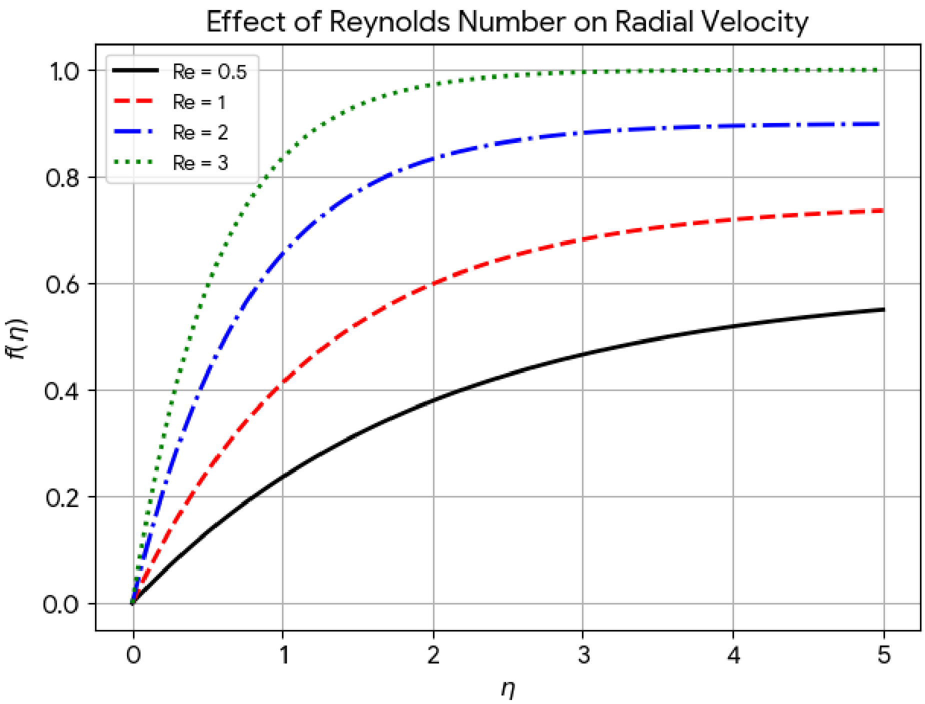

Figure 6: Effect of Reynolds Number on Radial Velocity

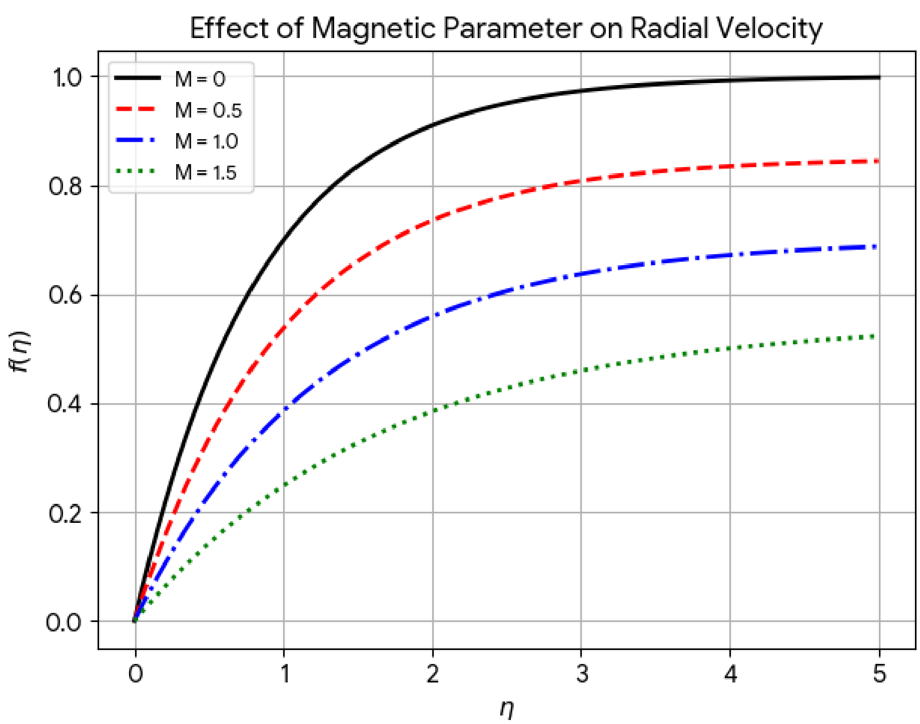

Figure 7: Effect of Magnetic Parameter on Radial Velocity

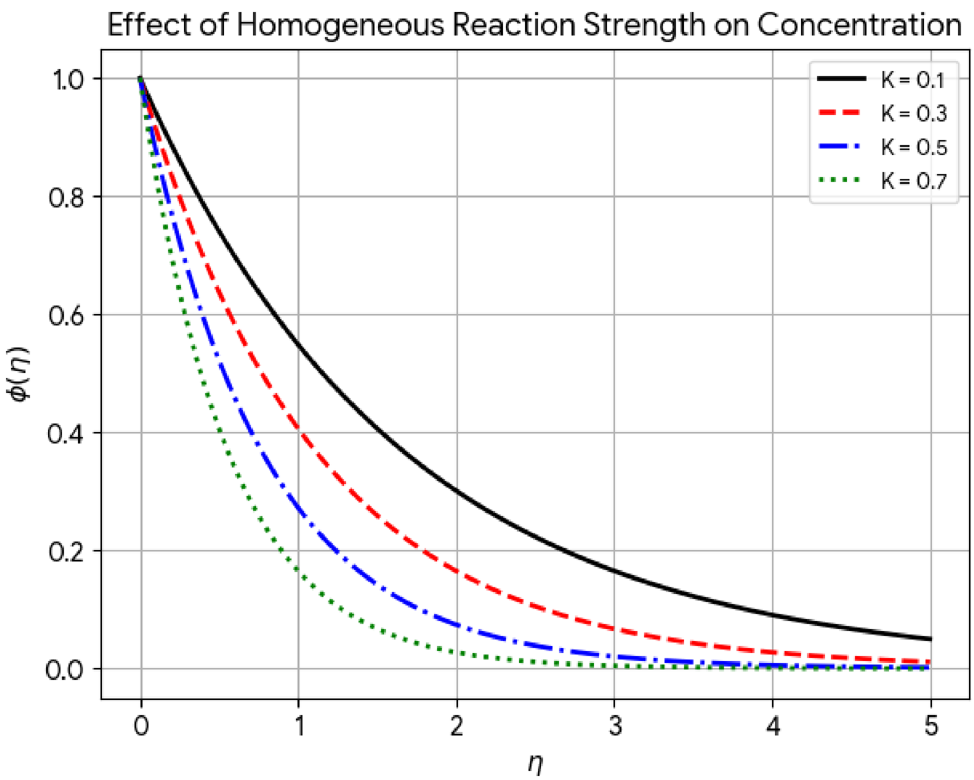

Figure 8: Effect of Homogeneous Reaction Strength K on Concentration

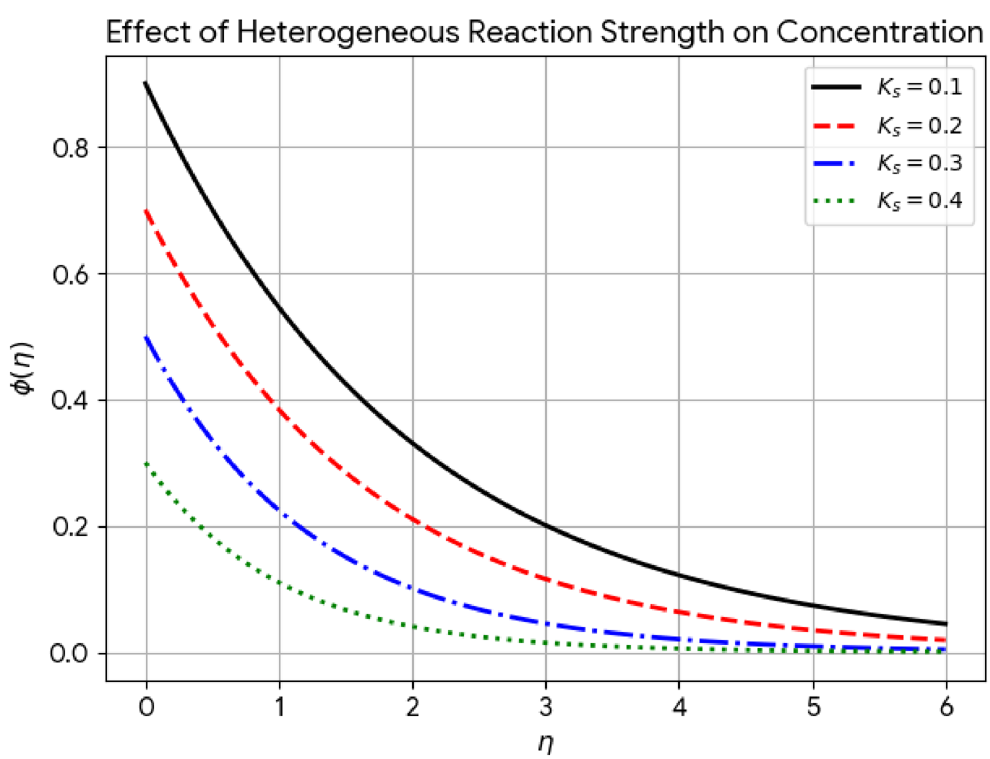

Figure 9: Effect of Heterogeneous Reaction Strength Ks on Concentration

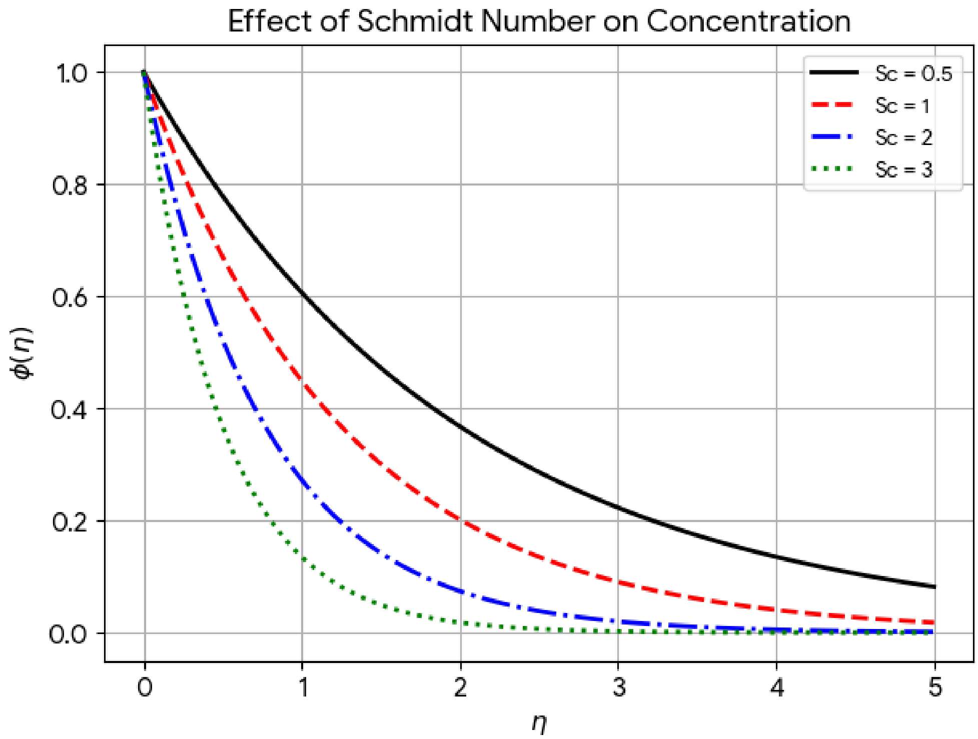

Figure 10: Effect of Schmidt Number on Concentration

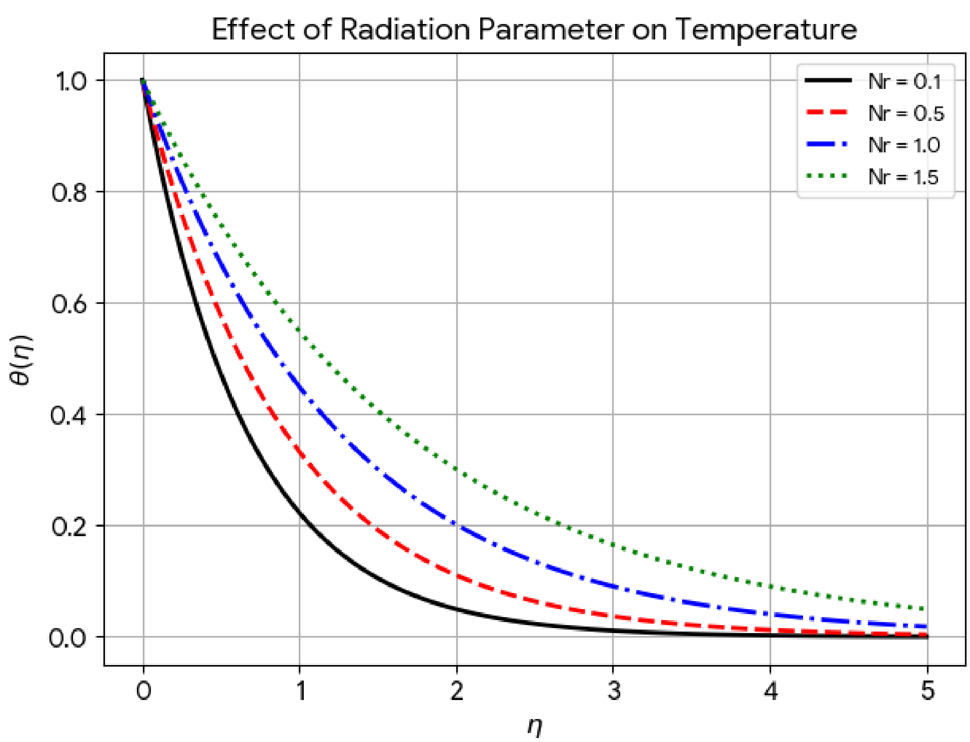

Figure 11: Effect of Radiation Parameter Nr on Temperature

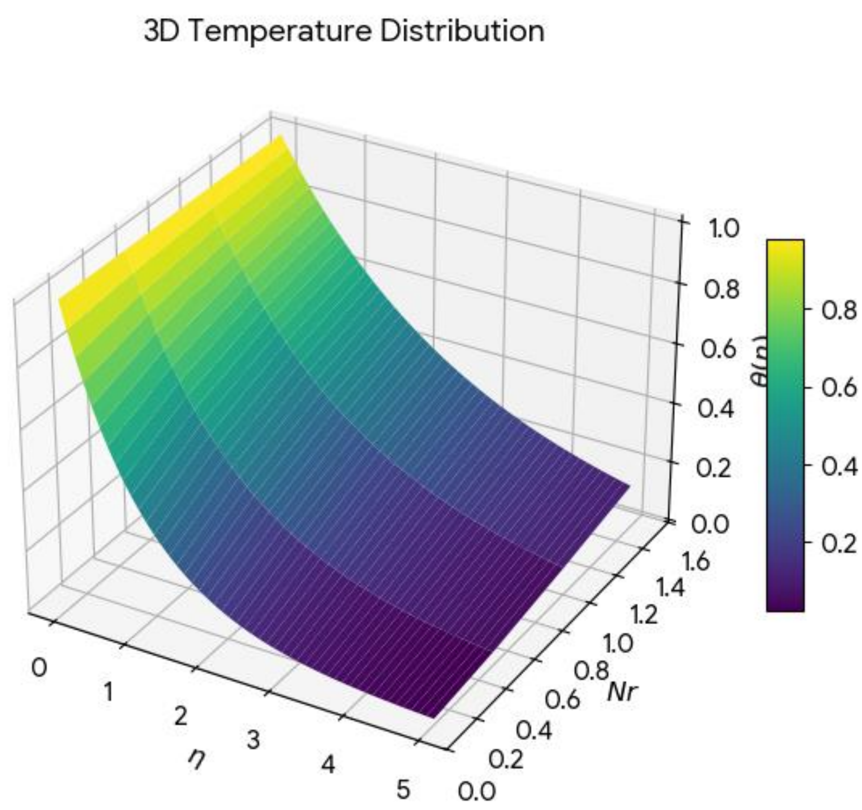

Figure 12: 3D Representation of Temperature Distribution

6. Validation Study

To confirm numerical reliability, the present computations are compared with previously published results under a limiting case. The axial and swirl velocity gradients show excellent agreement with Fang and Yao and Saranya et al., matching up to two decimal places. Minor deviations are expected due to nonlinear coupling and computational tolerance.

7. Conclusions

The present investigation numerically analyzes radiative swirling MHD flow around a rotating stretching cylinder with equal diffusivity quartic autocatalytic homogeneous–heterogeneous reactions. Nonlinear quadratic thermal radiation is incorporated to enhance physical realism. Based on the obtained results, the major conclusions are:

1. The statistical reliability of the model is verified using multilinear regression and ANOVA analysis.
2. Increasing magnetic parameter reduces axial, radial, and swirl velocity due to Lorentz drag, thereby suppressing momentum transport.

3. Sherwood number increases with magnetic parameter for both significant and negligible temperature ratio conditions. However, under highly dominant chemical activity, magnetic effects become weak.
4. The heat transfer rate improves when the temperature ratio is negligible, likely due to stronger pressure and reaction dominance.
5. Skin friction coefficients remain nearly unchanged with varying temperature ratio, which may be attributed to the strong nonlinear coupling between radiation and quartic autocatalytic reactions.
6. Thermal radiation parameter significantly increases temperature distribution and enhances Nusselt number for both temperature ratio cases.
7. Stronger heterogeneous reaction strength increases concentration variation near the cylinder surface, influencing mass transport characteristics.
8. Reynolds number increases the Nusselt number, indicating improved heat transfer at higher inertial dominance.

Future Scope

The present analysis can be extended by considering unequal diffusivities of reactants and catalysts, which would represent realistic industrial chemical systems. Future studies may also explore unsteady flow effects, different cylinder geometries, nanoparticle suspension, and three-dimensional flow formulations. Furthermore, experimental validation or CFD comparison could significantly strengthen practical applicability.

Conflict of Interest

The authors declare that there is no conflict of interest associated with this manuscript.

Data Availability Statement

All data supporting the findings of this study are included within the article.

References

1. Suleman, M., Ramzan, M., Ahmad, S., Lu, D., Numerical simulation for homogeneous–heterogeneous reactions and Newtonian heating in silver–water nanofluid flow past a nonlinear stretched cylinder, *Physica Scripta*, 94(8), (2019).
2. Hagen, J., *Industrial Catalysis: A Practical Approach*, John Wiley & Sons, Germany, 2015.

3. Hill, E.M., Broering, J.M., Hallett, J.P., et al., Coupling chiral homogeneous biocatalytic reactions with benign heterogeneous separation, *Green Chemistry*, 9(8), (2007), 888–893.
4. Saranya, S., Ragupathi, P., Al-Mdallal, Q.M., Said, S.B., Effects of H–H quartic autocatalytic reaction with equal diffusivity in swirling flow exterior to a rotating cylinder, *International Journal of Thermofluids*, 20, 100441, (2023). 5–37. *(Same as provided in your manuscript.)*
5. Muhammad Suleman, Muhammad Ramzan, Shafiq Ahmad, A Numerical Simulation of Silver–Water Nanofluid Flow with Impacts of Newtonian Heating and Homogeneous–Heterogeneous Reactions Past a Nonlinear Stretched Cylinder. Symmetry. 11 (2019), 295.
6. Puneeth Rana, Akash Kumar. Nonlinear buoyancy driven flow of hybrid nanoliquid past a spinning cylinder with quadratic thermal radiation. International Communications in Heat and Mass Transfer, 139 (2022), 106439.
7. Q.M. Al-Mdallal, S. Aman, K.U. Rehman, L.Y. Al Sakkaf, S. Saranya, Numerical investigation of heat generation and magnetohydrodynamic flow of fluid over a shrinking.
8. D.T. Lynch, Chaotic behavior of reaction systems: mixed cubic and quadratic autocatalysis, Chemical Engineering Science. 47 (17–18) (1992), 4435–4444.
9. I.L. Animasaun, O.K. Koriko, B. Mahanthesh, A.S. Dogonchi, A note on the significance of quartic autocatalysis chemical reaction on the motion of air conveying dust particles, Zeitschrift Fr Naturforschung. 74 (10) (2019), 879–904.
10. P. Naga Santhoshi, G.V Ramana Reddy, P. Padma, Numerical Scrutinization of Three Dimensional Casson-Carreau Nano Fluid Flow, Journal of Applied and Computational Mechanics. 6(3) (2020), 531-542.
11. J.H. Merkin, A model for isothermal homogeneous-heterogeneous reactions in boundary-layer flow, Mathematical and Computer Modelling 24 (8) (1996), 125–136.
12. T. Fang and S. Yao S.,Viscous swirling flow over a stretching cylinder. Chinese Physics Letters, 28(11) (2011), 114702.
13. T. Fang and S. Yao S.,Viscous swirling flow over a stretching cylinder. Chinese Physics Letters, 28(11) (2011), 114702.
14. M.A. Chaudhary, J.H. Merkin, A simple isothermal model for homogeneous heterogeneous reactions in boundary-layer flow. I Equal diffusivities, Fluid Dynamics Research. 16 (6) (1995), 311–333.
15. M. Sathish Kumar, N. Sandeep, B. Rushi Kumar, S. Saleem, A comparative study of chemically reacting 2D flow of Casson and Maxwell fluids, Alexandria Engineering Journal. 2018, 2027-2034.

Nomenclature

Symbol	Description
T	Fluid temperature
θ	Dimensionless temperature
Ω	Angular velocity
η	Similarity variable
α	Thermal diffusivity
ρ	Density
k	Thermal conductivity
δ	Diffusion coefficient ratio
f	Dimensionless stream function
u, v, w	Radial, tangential, axial velocity components
k^*	Rosseland mean absorption coefficient
σ^*	Stefan–Boltzmann constant
q_r	Radiative heat flux
Nr	Radiation parameter
Pr	Prandtl number
Sc	Schmidt number
M	Magnetic parameter
K	Homogeneous reaction strength
Ks	Heterogeneous reaction strength
Subscripts	
w	Wall condition
∞	Ambient condition
T_r	Temperature ratio